HHS Public Access

Author manuscript

Sci Transl Med. Author manuscript; available in PMC 2017 August 17.

Published in final edited form as:

Sci Transl Med. 2017 June 28; 9(396): . doi:10.1126/scitranslmed.aak9969.

Genetic and epigenetic inactivation of *SESTRIN1* controls mTORC1 and response to EZH2 inhibition in follicular lymphoma

Elisa Oricchio[1,*], **Natalya Katanayeva**[1], **Maria Christine Donaldson**[1], **Stephanie Sungalee**[1], **Joyce P. Pasion**[2], **Wendy Béguelin**[3], **Elena Battistello**[1,4], **Viraj R. Sanghvi**[2], **Man Jiang**[2], **Yanwen Jiang**[5], **Matt Teater**[5], **Anita Parmigiani**[6], **Andrei V. Budanov**[6,7], **Fong Chun Chan**[8,9], **Sohrab P. Shah**[10,11], **Robert Kridel**[8,12], **Ari M. Melnick**[3], **Giovanni Ciriello**[4], and **Hans-Guido Wendel**[2]

[1]Swiss Institute for Experimental Cancer Research (ISREC), School of Life Sciences, École Polytechnique Fédérale de Lausanne (EPFL), 1015 Lausanne, Switzerland [2]Cancer Biology and Genetics Program, Memorial Sloan Kettering Cancer Center, New York, NY 10065, USA [3]Division of Hematology/Oncology, Weill Cornell Medical College, Cornell University, 1300 York Avenue, New York, NY 10065, USA [4]Department of Computational Biology, University of Lausanne, 1005 Lausanne, Switzerland [5]Institute for Computational Biomedicine, Weill Cornell Medical College, Cornell University, New York, NY 10065, USA [6]Department of Human and Molecular Genetics, Goodwin Research Laboratories, Massey Cancer Center, Virginia Commonwealth University, Richmond, VA 23298, USA [7]School of Biochemistry and Immunology, Trinity Biomedical Sciences Institute, Trinity College Dublin, Pearse Street, Dublin 2, Ireland [8]Centre for Lymphoid Cancer, BC Cancer Agency, Vancouver, British Columbia V5Z 1L3, Canada [9]Bioinformatics Graduate Program, University of British Columbia, Vancouver, British Columbia, Canada [10]Department of Pathology and Laboratory Medicine, University of British Columbia, Vancouver, British Columbia, Canada [11]Department of Molecular Oncology, BC Cancer Agency, Vancouver, British Columbia, Canada [12]Division of Medical Oncology and Hematology, Princess Margaret Cancer Centre, Toronto, Ontario, Canada

Abstract

[*]Corresponding author. elisa.oricchio@epfl.ch.

Author contributions: E.O. and N.K. conducted experiments and were involved in the experimental design and data analysis. M.J. and E.B. assisted with experiments. M.C.D. performed the Western blots for histone methylation marks. S.S. analyzed the ChIP-seq data. J.P.P. conducted the treatment experiment with mTOR inhibitor. V.R.S. designed and cloned CRISPRs. W.B. analyzed the GCB-DLBCL patient expression data. Y.J. and M.T. analyzed the expression data in FL patients. R.K., F.C.C., and S.P.S. provided FL samples for mutually exclusive analysis. A.M.M. supervised the expression analysis in primary DLBCL and FL patients and discussed the results. A.V.B. and A.P. provided Sestrin1 antibody and analyzed Sestrin1 expression by Western blot. G.C. designed and performed computational analyses. E.O. designed the study. E.O. and H.-G.W. wrote the paper.

Competing interests: A.M. is a consultant for Epizyme. The other authors declare that they have no competing interests.

Data and materials availability: The data for this study are available in the Gene Expression Omnibus database at accession numbers GSE40989, GSE12195, and GSE40971.

SUPPLEMENTARY MATERIALS

www.sciencetranslationalmedicine.org/cgi/content/full/9/396/eaak9969/DC1

Materials and Methods

References (37–43)

Follicular lymphoma (FL) is an incurable form of B cell lymphoma. Genomic studies have cataloged common genetic lesions in FL such as translocation t(14;18), frequent losses of chromosome 6q, and mutations in epigenetic regulators such as *EZH2*. Using a focused genetic screen, we identified *SESTRIN1* as a relevant target of the 6q deletion and demonstrate tumor suppression by *SESTRIN1* in vivo. Moreover, *SESTRIN1* is a direct target of the lymphoma-specific *EZH2* gain-of-function mutation ($EZH2^{Y641X}$). *SESTRIN1* inactivation disrupts p53-mediated control of mammalian target of rapamycin complex 1 (mTORC1) and enables mRNA translation under genotoxic stress. *SESTRIN1* loss represents an alternative to *RRAGC* mutations that maintain mTORC1 activity under nutrient starvation. The antitumor efficacy of pharmacological EZH2 inhibition depends on SESTRIN1, indicating that mTORC1 control is a critical function of EZH2 in lymphoma. Conversely, $EZH2^{Y641X}$ mutant lymphomas show increased sensitivity to RapaLink-1, a bifunctional mTOR inhibitor. Hence, SESTRIN1 contributes to the genetic and epigenetic control of mTORC1 in lymphoma and influences responses to targeted therapies.

INTRODUCTION

Genetic and epigenetic alterations in cancer point to the biological processes driving tumor development and may reveal opportunities for therapy (1). Follicular lymphoma (FL) is among the most common forms of indolent B cell lymphoma, and cytogenetic studies have identified the chromosomal translocation t(14;18), which activates the anti-apoptotic *BCL2* gene, as a hallmark of the disease (2). Recent sequencing studies have cataloged somatic mutations in FL. These include frequent mutations in epigenetic regulators such as *KMT2D*, *CREBBP*, and EZH2 (3–7), immune receptor genes such as *TNFRSF14*, *CD79B*, and *B2M* (8–10), and somewhat less frequent mutations in mammalian target of rapamycin complex 1 (mTORC1) regulators such as *RAGGC* and *ATP6V1B2* (11).

FLs also harbor recurrent copy number changes, and the exact genetic targets of large chromosomal lesions can be difficult to define. For example, deletions of chromosome (Chr.) 6q occur in about 25 to 30% of FLs, which have been linked to poor prognosis (12, 13). The tumor suppressor genes *A20/TNFAIP3* (14) and ephrin receptor A7 (*EPHA7*) (15) have been identified as targets of the Chr. 6q deletions. However, the size and complexity of Chr. 6q lesions suggest the presence of additional genetic targets. Unbiased genetic screens provide an efficient way to pinpoint candidate tumor suppressor genes within large chromosomal lesions (15, 16). Here, we identified the mTORC1 regulator *SESTRIN1* (17–20) as a tumor suppressor and treatment response modifier in FL.

RESULTS

SESTRIN1 is a functional target of Chr. 6q deletions in FL

A meta-analysis of copy number data from two large cohorts of indolent FLs [Memorial Sloan Kettering Cancer Center (MSKCC), $n = 64$; University of Nebraska Medical Center (UNMC), $n = 196$] (GSE40989) (21, 22) shows copy number losses at Chr. 6q in 34% (89 of 260) of the analyzed cases (Fig. 1A and fig. S1A). GISTIC analysis (23) identifies one peak on Chr. 6p21 and five significant [false discovery rate (FDR) < 0.01] and frequently altered

regions on Chr. 6q: Chr. 6q13, Chr. 6q14, Chr. 6q16-21, Chr. 6q23, and Chr. 6q27 (Fig. 1B and table S1). The frequency of homozygous and heterozygous deletions is similar in the different regions, varying between 9 and 13% for the homozygous and between 12 and 16% for the heterozygous (Fig. 1C and table S2). Moreover, we identified individual samples harboring rare but highly focal events (<5 Mb). These focal deletions are larger than commonly described germline variants, and they are not listed in the database of genomic variants (http://dgv.tcag.ca), indicating that they are tumor-specific and may target functionally relevant genes associated with FL development (table S3). For example, we identified focal losses targeting *TNFAIP3*/*A20* and *SESTRIN1* (Fig. 1D), suggesting that *SESTRIN1* may be a target of the Chr. 6q deletion in FL. However, despite this focal alteration, most of the deletions targeting *SESTRIN1* are large and simultaneously also affect other genes including, for example, *PRDM1*.

To identify functionally relevant targets of the Chr. 6q deletions, we performed unbiased RNA interference (RNAi) focused on genes encoded at Chr. 6q. We screened 81 genes [each gene was targeted by one to six short hairpin RNAs (shRNAs)] for enhanced viability in immortalized pro—B cells (FL5-12) that depend on interleukin-3 (IL-3) (fig. S1B) (15, 24). FL5-12 pro—B cells represent a different phase of B cell differentiation than B cells in FL tumors; however, they are a useful in vitro model to screen for genetic modifiers that need to be further explored in a relevant in vivo model of lymphomagenesis (25, 26). In our screen, we identified 29 shRNAs enriched at least 1.5-fold, indicating a survival advantage in IL-3—depleted FL5-12 cells (table S4). As expected, these included shRNAs against the tumor suppressor genes *Epha7* (15) and *Tnfaip3* (14). In addition, two of three shRNAs targeting *Sestrin1* scored positively in our screen, with fold change greater than 1.5 ($P = 0.02$) (fig. S1C). We confirmed their ability to significantly ($P = 0.01$) down-regulate *Sestrin1* expression (fig. S1D), promote IL-3—independent survival (Fig. 1E), and accelerate proliferation (fig. S1E). Thus, *Sestrin1* reduction enhances pro—B cell survival and indicates a potential tumor suppressor function.

Deficiency of *Sestrin1* promotes FL development in vivo

We used the vavBcl2 model of FL to directly test the effect of *Sestrin1* deficiency on lymphoma development. This model recapitulates key aspects of the genetics and pathology of human FL (15, 27). We transduced vavBcl2 hematopoietic precursor cells (HPCs) with empty vector MSCV-IRES-GFP or with the two shRNAs targeting *Sestrin1* pinpointed by the screen, and we transplanted the modified vavBcl2 HPCs into lethally irradiated, syngeneic, wild-type animals (Fig. 2A). In recipient mice, knockdown of *Sestrin1* resulted in significant acceleration of lymphoma development (sh-1 *Sestrin1:* $n = 10$; median survival, 93 days; log-rank P = 0.041; sh-2 *Sestrin1:* $n = 12$; median survival, 82 days; log-rank $P = 0.028$) (Fig. 2B). The shRNAs selectively down-regulated *Sestrin1* expression and did not affect *Sestrin2* or *Sestrin3* (Fig. 2, C and D). Surface marker and pathological analyses confirmed the similarity of control and *Sestrin1*-deficient murine lymphomas with human FLs. For example, we found the pathognomonic follicular structure, lack of apoptosis by TUNEL (terminal deoxynucleotidyl transferase—mediated deoxyuridine triphosphate nick end labeling), expression of the germinal center (GC) markers peanut agglutinin (PNA) and BCL6, somatic hypermutation in the VDJH4 variable region, and a predominant $B220^+$ and

$CD19^+$ B cell population with modest infiltration of $CD4^+$ or $CD8^+$ T cells in both controls and tumors expressing shRNAs targeting *Sestrin1* (Fig. 2E and fig. S2, A to C). Although the Ki67-positive staining is low as in the human disease, loss of *Sestrin1* significantly increases tumor proliferation [average of the number of Ki67-positive cells in control = 8.5%, sh-2 *Sestrin1* = 23.1% ($P = 0.02$), and sh1 *Sestrin1* = 15.5% ($P = 0.05$)] (Fig. 2E and fig. S2D). Consistent with Sestrin's function as an upstream regulator of mTORC1 (18–20), we found increased phosphorylation of eukaryotic translation initiation factor 4E—binding protein 1 (4EBP1) and ribosomal S6 protein by immunohistochemistry (Fig. 2F and fig. S2,E and F)and immunoblots of Sestrin1-deficient lymphoma cells compared to the control (Fig. 2G). Hence, Sestrin1 acts a tumor suppressor that controls mTORC1 activity in an animal model of FL.

SESTRIN1 is a direct target of repression by $EZH2^{Y641X}$ in lymphoma

We examined the expression of *SESTRIN1* in human B cells and in FL and diffuse large B cell lymphoma (DLBCL) samples. *SESTRIN1* expression is similar in naïve and memory B cells, centroblasts, centrocytes, FL, and DLBCL (fig. S3A) (GSE12195). By subdividing the tumor samples based on *EZH2* mutation status, we noticed a significant reduction of *SESTRIN1* expression in FL tumor samples that carried the EZH2 gain-of-function mutation ($EZH2^{Y641X}$; $n = 5$) compared to samples that were *EZH2* wild type ($n = 52$; $P = 0.0038$) (Fig. 3A). We further observed the same significant association between *SESTRIN1* expression and mutant $EZH2^{Y641X}$ in GC-type DLBCL ($EZH2^{Y641X}$, $n = 8$; *EZH2* wild type, $n = 30$; $P = 0.022$) (Fig. 3B and table S5) (28, 29). Expression of *SESTRIN2* and *SESTRIN3* was not related to *EZH2* mutation status in either FL or DLBCL samples (fig. S3, B to E). Chromatin immunoprecipitation—quantitative polymerase chain reaction (ChIP-qPCR) using three separate probes covering the *SESTRIN1* promoter revealed a significant ($P \leq 0.01$) enrichment of EZH2 on *SESTRIN1* promoter (Fig. 3C and fig. S3F) associated with an increase of H3K27me3 in $EZH2^{Y641X}$ mutated compared to *EZH2* wild-type cells in the same region (Fig. 3D and fig. S3G). Hence, expression of *SESTRIN1* is linked to the activity of the mutant $EZH2^{Y641X}$ polycomb protein in lymphoma samples.

We directly tested the effect of EZH2 inhibition on *SESTRIN1* gene expression across a panel of cell lines. Gene expression data from lymphoma cell lines of *EZH2* wild type ($n = 2$) or $EZH2^{Y641X}$ mutant ($n = 6$) confirmed a significant loss of *SESTRIN1* expression in $EZH2^{Y641X}$ mutant lines (FDR < 0.01; $P = 8.86 \times 10^{-8}$) (Fig. 3E and table S6) (GSE40971) comparable to the down-regulation observed in previously reported targets of EZH2 (fig. S3H) (30). Global level of H3K27me3 is higher in $EZH2^{Y641X}$ mutant than in the *EZH2* wild-type cells, and treatment with the EZH2 inhibitor caused loss of the H3K27me3 mark (fig. S3I). This change in the histone mark corresponded to a significant ($P \leq 0.01$) increase in *SESTRIN1* mRNA and protein expression in the $EZH2^{Y641X}$ mutant cells (Fig. 3, E and F, and fig. S3J), whereas it had no effect on *SESTRIN1* expression in EZH2 wild-type lines (Fig. 3, F and G, and table S7). To allay potential concerns about drug selectivity, we confirmed that RNAi-mediated *EZH2* knockdown in *EZH2* mutant Karpas-422 cells caused induction of the *SESTRIN1* mRNA (fig. S3K) (GSE41239), and we obtained similar results using an additional EZH2 inhibitor, EPZ-6438, in a panel of *EZH2* wild-type and mutant lymphoma cells (fig. S3L). ChIP demonstrated a significant ($P < 0.05$) GSK126-sensitive

association of the *SESTRIN1* promoter with the H3K27me3 mark (Fig. 3H). We performed ChIP-qPCR for the H3K27me3 mark and histone-3 in *EZH2*^{Y641X} mutant SU-DHL-6 cells treated with GSK126, showing an association with the *SESTRIN1* promoter but not the *RPL30* or *TNFAIP3* promoter used as controls (Fig. 3H and fig. S3M). An analysis of promoter methylation and *SESTRIN1* sequence in 15 primary FL samples and five cell lines did not reveal aberrant CpG island methylation or mutations (fig. S3N). Hence, the mutant polycomb factor EZH2^{Y641X} controls SESTRIN1 expression in lymphoma cells.

Next, we explored the genetic relationship between *SESTRIN1* deletions, mutation status of *EZH2*, and recently reported RAG C guanosine triphosphatase (GTPase) (*RRAGC*) mutations that also act to increase mTORC1 activity (11). The analysis of 172 FL samples revealed a significant mutually exclusive relationship between alterations in *EZH2*, *RRAGC*, and *SESTRIN1* ($P = 0.03$), which affect 47% of the cases (fig. S3O). Moreover, an analysis focused only on the relationship between *SESTRIN1* loss and *EZH2* mutations was performed across multiple data sets, including 172 FL and 88 DLBCL (31, 32). Thirty-five percent of the cases (92 of 260) harbor either *EZH2* mutations or *SESTRIN1* loss, and only six cases show concurrent alteration of both genes ($P = 0.06$) (fig. S3P). Together, these data indicate that SESTRIN1, RRAGC, and EZH2 lesions are alternate events implicated in mTORC1 control in lymphoma.

Mutant EZH2^{Y641X} activates mTORC1 and mRNA translation in lymphoma

SESTRIN family of proteins control mTORC1 activity in response to p53 activation and reduce mRNA translation in response to DNA damage (17–19, 33). Therefore, we examined the cellular response to DNA damage in the presence of the *EZH2*^{Y641X} gain-of-function mutation. We treated OCI-LY19 and SU-DHL-5 cells (wild type for *p53* and *EZH2*) and SU-DHL-10 and VAL cells (*p53* wild type and *EZH2*^{Y641X}) (table S8) with the topoisomerase-2 inhibitor doxorubicin (DXR; 200 nM). This treatment failed to induce *SESTRIN1* expression in *EZH2*^{Y641X} mutant cells, whereas both *EZH2* wild-type and mutant cell lines responded with induction of *SESTRIN2* and *p21* mRNAs (Fig. 4A and fig.S4A). Consistently, DXR caused an inhibition of mTORC1 signaling, as indicated by loss of phosphorylation of 4E-BP and ribosomal S6 in wild-type cells but not in *EZH2*^{Y641X} mutant cells (Fig. 4B and fig. S4, B and C; quantified in fig. S4, D and E). Hence, the *EZH2*^{Y641X} gain-of-function mutation can override mTORC1 inhibition caused by genotoxic stress in lymphoma cells by inhibiting *SESTRIN1*.

Next, we wondered whether the epigenetic control of mTORC1 strictly depends on SESTRIN1 or whether there is a backup mechanism. Treatment with the EZH2 inhibitor, GSK126, blocked mTORC1 signaling in *EZH2*^{Y641X} mutant cells (SU-DHL-10, SU-DHL-6, and Karpas-422) as indicated by loss of ribosomal S6 and 4E-BP phosphorylation (Fig. 4C and fig. S4F). By contrast, *SESTRIN1* isogenic deficient cells generated using clustered regularly interspaced short palindromic repeats (CRISPR)/Cas9 or shRNAs showed no effect on mTORC1 activity (Fig. 4D and fig. S4, G and H). Moreover, metabolic labeling of nascent protein production with a methionine synthetic analog [L-azidohomoalanine (AHA)] revealed that *SESTRIN1*-proficient lymphoma cells readily reduced translation rates by 23%, whereas *SESTRIN1*-defective lymphoma cells were

unable to reduce translation in response to EZH2 inhibition; rapamycin was used as control, and, as expected, it showed equal translation inhibition independent of SESTRIN1 (Fig. 4, E and F). Hence, SESTRIN1 is an important node that links EZH2 and the control of mTORC1 and mRNA translation.

Therapeutic EZH2 inhibition depends on SESTRIN1

The mutant $EZH2^{Y641X}$ protein can potentially control a large number of genes, and it is not clear which of these are required for response to an EZH2 inhibitor. We assessed the relative importance of SESTRIN1 by treating isogenic SESTRIN1-competent and SESTRIN1-deficient lymphoma cells with GSK126. Treatment of *EZH2*^{Y641X} mutant SU-DHL-10 cells with GSK126 readily induced cell death in the parental line, whereas *SESTRIN1* inactivation in the same cells prevented cell death (fig. S4, I and J). Next, we directly compared the in vivo response of isogenic pairs of *SESTRIN1*-proficient (SU-DHL-10 vector) and *SESTRIN1*-deficient (SU-DHL-10 CRISPR-Sestrin1) lymphomas to EZH2 inhibition. We xenografted lymphomas into the right and left flanks of immunodeficient (NOD.CB17-Prkdc^{scid}) mice. We initiated treatment with EZH2 inhibitor (GSK126) [75 mg/kg intraperitoneally (ip) daily for 14 days] or vehicle once tumors had reached a size of 5 to 10 mm^3. In *SESTRIN1*-proficient tumors, GSK126 caused a significant ($P = 0.013$) growth reduction compared to vehicle (Fig. 4G); in contrast, the *SESTRIN1*-deficient tumors failed to respond to the EZH2 inhibitor (Fig. 4, H and I). Tumor analyses by immunohistochemistry and immunoblots readily showed differential induction of apoptosis by cleaved caspase3 and differential inhibition of mTORC1 activity by phosphorylation of ribosomal S6 and 4E-BP1 proteins between SESTRIN1-proficient and SESTRIN1-deficient tumors (Fig. 4J and fig. S4, K and L). These results indicate that mutated EZH2 controls mTORC1 activity through SESTRIN1 in lymphoma.

We have seen that mutant *EZH2* can override the p53-mediated induction of *SESTRIN1*. We now wondered whether EZH2 inhibition and *SESTRIN1* expression also contribute to DNA damage response induced by chemotherapeutic agents. We pretreated SU-DHL-10 lymphoma cells with the EZH2 inhibitor (GSK126, 2 μM) for 1 day, and then we added DXR for an additional day (DXR, 50 nM). Pretreatment with the EZH2 inhibitor reduced mTORC1 activity, as indicated by a decrease in phospho-S6, but did not significantly enhance the antiproliferative effect of DXR in vitro (fig. S4, M and N).

EZH2 mutant lymphomas are sensitive to a bifunctional mTOR inhibitor

EZH2 mutant lymphoma cells show down-regulation of *SESTRIN1 and* mTORC1 activation. We wondered whether these tumors were also more sensitive to pharmacological mTORC1 inhibition. RapaLink-1 is a third-generation mTORC1 inhibitor that binds both the FRB (FKBP-rapamycin binding) and the mTORC kinase domains and therefore combines the mTORC1 selectivity of rapamycin with the better target inhibition of mTOR kinase inhibitors (Fig. 4K) (34). We treated a panel of *EZH2* wild-type (OCI-LY19, Toledo, and DoHH2) and *EZH2* mutant (SU-DHL-10, SU-DHL-4, and SU-DHL-6) lymphoma cell lines with low (12.5 nM) and high (50 nM) dose of RapaLink-1 for 48 hours. *EZH2* mutant cells were more sensitive to this inhibitor than *EZH2* wild-type lines. Specifically, we observed cell death induction in 80 to 95% of *EZH2*^{Y641X} mutant cells compared to 10 to 70% of

$EZH2^{WT}$ cells for both low and high drug concentrations (Fig. 4L and fig. S4O). These results indicate specific pharmacological vulnerabilities of *$EZH2^{Y641X}$* mutant lymphomas.

DISCUSSION

SESTRIN1 is a known regulator of mTORC1 that is transcriptionally induced by p53 upon DNA damage and mediates cell growth inhibition upon genotoxic stress (17–19). Our study identifies the *SESTRIN1* gene as a bona fide tumor suppressor in lymphoma and a biologically relevant target of the frequent Chr. 6q deletions that are observed in ~20% of human lymphomas. These chromosomal deletions are typically large and encompass several genes, including previously reported tumor suppressors in lymphoma such as *TNFAIP3*, *EPHA7*, and *PRDM1* (14, 15, 35). *SESTRIN1* is rarely focally deleted and could thus be missed when considering genomic data alone. Nonetheless, through complementary functional analyses using a chimeric mouse model of lymphoma, we could demonstrate the importance of *SESTRIN1* in FL development.

In addition to chromosomal loss, *SESTRIN1* is epigenetically silenced by the lymphoma-specific mutant $EZH2^{Y641X}$, resulting in mTORC1 activation in lymphoma. *SESTRIN1* is not a target of mutations, in contrast to the *RRAGC*, which is mutated in 7% of FLs (11). Mutations in *EZH2* and *RRAGC* and loss of *SESTRIN1* show a mutually exclusive relationship, indicating that they are alternate paths to maintain mTORC1 activity under conditions that would otherwise shut down cell growth. The combined frequency of these lesions (47% of examined cases of FL and DLBCL) indicates that maintaining active mTORC1 signaling is an important biological requirement in a large group of lymphomas. There are functional differences between SESTRIN1 and RRAGC. Although SESTRIN1 controls the Rag GTPases RAG A and RAG B in response to genotoxic stress (19, 20), RRAGC encodes for the RAG C protein that, together with RAG D, mediates nutrient-sensitive mTORC1 control (36). However, mutual exclusivity between RRAGC and SESTRIN1 alterations indicates that either lesion is sufficient to maintain mTORC1 in lymphoma cells.

The polycomb factor EZH2 is a target of activating mutations in 7 to 20% of human FLs, promoting increase in H3K27me3 genome-wide and thus targeting several genes. We showed that *SESTRIN1* is an important $EZH2^{Y641X}$ target, and it may influence therapeutic response to EZH2 inhibitors like GSK126. Our findings show that EZH2 controls mTORC1 through SESTRIN1, and this epigenetic control can override p53 and DNA damage—induced mTORC1 blockade. We further find that SESTRIN1 reactivation and mTORC1 control are important downstream effects of *EZH2* gain-of-function mutations. This is supported by the genetic relationship between these lesions and experimental data showing that *SESTRIN1* loss protects against EZH2 inhibition. Although we do not have direct clinical evidence and it is difficult to test the efficacy of EZH2 inhibitors on primary FL samples because of their limited ability to grow in vitro, these results suggest that *SESTRIN1* deletions may predict reduced efficacy of EZH2 inhibitor treatment in lymphoma. Conversely, our results reveal that EZH2-mediated epigenetic down-regulation of *SESTRIN1* increases the dependency of lymphomas on mTORC1 and induces sensitivity to mTORC1 inhibitors in EZH2 mutant lymphomas. Together, our study establishes an

epigenetic mechanism of mTORC1 control and suggests that SESTRIN1 status should have an impact on the response to lymphoma therapeutics.

MATERIALS AND METHODS

Study design

This study was designed to identify tumor suppressor genes in FL that are targeted by chromosomal deletions and/or epigenetically silenced. Initially, we analyzed array comparative genomic hybridization data (aCGH) for 260 FL patients and used an shRNA screen in murine pro—B cells (as a surrogate model) to identify genes that control B cell proliferation. We confirmed the screen results in pro—B cells and in a murine model of FL (vavP-Bcl2) (Figs. 1 and 2). We calculated the minimum number of animals needed to observe significant differences in the survival curve by power analysis. In the second part of the study (Figs. 3 and 4), we focused on epigenetic regulation. We analyzed expression data in FL and GC-DLBCL patient samples that were $EZH2^{WT}$ or $EZH2^{Y641X}$. We selected patients harboring $EZH2^{Y641X}$ mutations; we excluded a cell line with UTX mutations and patients harboring different mutations for EZH2. To confirm a direct effect of mutated EZH2 on H3K27me3, we compared H3K27me3 ChIP at the gene-specific locus in mutant or wild-type EZH2 cells. To compare different responses to the EZH2 inhibitor (GSK126), we used genetically modified cells. Syngeneic cells were transplanted subcutaneously, and tumor size was determined by direct measurement of the tumors. We selected animals with similar tumor size and randomly assigned them to untreated and treated groups. The number of replicates and the statistical analyses are reported in the figure legends and below.

Statistical analysis

Significant differences in mRNA expression measured by RNA sequencing (fragments per kilobase of transcript per million) were determined by Wilcoxon rank test. Differential expression analyses on microarray data were performed using the Limma R package. Significant differences in expression measured by qPCR were determined by one- or two-tailed t test as reported in each figure legend. Statistical significance of mutual exclusivity was determined by random permutation tests ($n = 1000$). The bar graphs show the mean and SD or SEM as indicated in the figure legends. The exact P values are reported in each figure, and n.s. stands for non—statistically significant ($P > 0.05$).

Supplementary Material

Refer to Web version on PubMed Central for supplementary material.

Acknowledgments

We thank the laboratories of M. Li and M. Peng (MSKCC), as well as D. Hanahan [Swiss Institute for Experimental Cancer Research—École Polytechnique Fédérale de Lausanne (ISREC-EPFL)], for sharing reagents, F. Martinon (University of Lausanne) and F. Bertoni (Istituto Oncologico della Svizzera Italiana) for sharing lymphoma cell lines, the Memorial Sloan Kettering and EPFL research animal facilities, and the pathology and flow cytometry core facilities.

Funding: This work is supported by grants from the ISREC Foundation (to E.O.), Anna Fuller Fund (to E.O.), Swiss National Science Foundation (to E.O.), and Giorgi-Cavaglieri Foundation (to G.C.). A.V.B. is supported by

the National Cancer Institute grant (CA172660). H.-G.W. is supported by the Lymphoma Research Foundation; Mr. William H. Goodwin and Mrs. Alice Goodwin and the Commonwealth Foundation for Cancer Research; the Center for Experimental Therapeutics at MSKCC; NIH grants RO1CA183876-01, R01CA207217-01, R01CA19038-01, and P50CA192937-01A1; the Starr Cancer Consortium; the Geoffrey Beene Cancer Research Center; a Leukemia and Lymphoma Society (LLS) SPORE grant; and the MSKCC Core Grant (P30 CA008748). H.-G.W. is a scholar of the LLS. R.K. is supported by the Princess Margaret Cancer Centre start-up fund.

REFERENCES AND NOTES

1. Kelly TK, De Carvalho DD, Jones PA. Epigenetic modifications as therapeutic targets. Nat Biotechnol. 2010; 28:1069–1078. [PubMed: 20944599]
2. Haldar S, Beatty C, Tsujimoto Y, Croce CM. The bcl-2 gene encodes a novel G protein. Nature. 1989; 342:195–198. [PubMed: 2478890]
3. Okosun J, Bödör C, Wang J, Araf S, Yang C-Y, Pan C, Boller S, Cittaro D, Bozek M, Iqbal S, Matthews J, Wrench D, Marzec J, Tawana K, Popov N, O'Riain C, O'Shea D, Carlotti E, Davies A, Lawrie CH, Matolcsy A, Calaminici M, Norton A, Byers RJ, Mein C, Stupka E, Lister TA, Lenz G, Montoto S, Gribben JG, Fan Y, Grosschedl R, Chelala C, Fitzgibbon J. Integrated genomic analysis identifies recurrent mutations and evolution patterns driving the initiation and progression of follicular lymphoma. Nat Genet. 2013; 46:176–181. [PubMed: 24362818]
4. Morin RD, Johnson NA, Severson TM, Mungall AJ, An J, Goya R, Paul JE, Boyle M, Woolcock BW, Kuchenbauer F, Yap D, Humphries RK, Griffith OL, Shah S, Zhu H, Kimbara M, Shashkin P, Charlot JF, Tcherpakov M, Corbett R, Tam A, Varhol R, Smailus D, Moksa M, Zhao Y, Delaney A, Qian H, Birol I, Schein J, Moore R, Holt R, Horsman DE, Connors JM, Jones S, Aparicio S, Hirst M, Gascoyne RD, Marra MA. Somatic mutations altering EZH2 (Tyr641) in follicular and diffuse large B-cell lymphomas of germinal-center origin. Nat Genet. 2010; 42:181–185. [PubMed: 20081860]
5. Morin RD, Mendez-Lago M, Mungall AJ, Goya R, Mungall KL, Corbett RD, Johnson NA, Severson TM, Chiu R, Field M, Jackman S, Krzywinski M, Scott DW, Trinh DL, Tamura-Wells J, Li S, Firme MR, Rogic S, Griffith M, Chan S, Yakovenko O, Meyer IM, Zhao EY, Smailus D, Moksa M, Chittaranjan S, Rimsza L, Brooks-Wilson A, Spinelli JJ, Ben-Neriah S, Meissner B, Woolcock B, Boyle M, McDonald H, Tam A, Zhao Y, Delaney A, Zeng T, Tse K, Butterfield Y, Birol I, Holt R, Schein J, Horsman DE, Moore R, Jones SJM, Connors JM, Hirst M, Gascoyne RD, Marra MA. Frequent mutation of histone-modifying genes in non-Hodgkin lymphoma. Nature. 2011; 476:298–303. [PubMed: 21796119]
6. Green MR, Kihira S, Liu CL, Nair RV, Salari R, Gentles AJ, Irish J, Stehr H, Vicente-Dueñas C, Romero-Camarero I, Sanchez-Garcia I, Plevritis SK, Arber DA, Batzoglou S, Levy R, Alizadeh AA. Mutations in early follicular lymphoma progenitors are associated with suppressed antigen presentation. Proc Natl Acad Sci USA. 2015; 112:E1116–E1125. [PubMed: 25713363]
7. Zhang J, Dominguez-Sola D, Hussein S, Lee JE, Holmes AB, Bansal M, Vlasevska S, Mo T, Tang H, Basso K, Ge K, Dalla-Favera R, Pasqualucci L. Disruption of KMT2D perturbs germinal center B cell development and promotes lymphomagenesis. Nat Med. 2015; 21:1190–1198. [PubMed: 26366712]
8. Cheung KJJ, Johnson NA, Affleck JG, Severson T, Steidl C, Ben-Neriah S, Schein J, Morin RD, Moore R, Shah SP, Qian H, Paul JE, Telenius A, Relander T, Lam W, Savage K, Connors JM, Brown C, Marra MA, Gascoyne RD, Horsman DE. Acquired TNFRSF14 mutations in follicular lymphoma are associated with worse prognosis. Cancer Res. 2010; 70:9166. [PubMed: 20884631]
9. Pasqualucci L, Trifonov V, Fabbri G, Ma J, Rossi D, Chiarenza A, Wells VA, Grunn A, Messina M, Elliot O, Chan J, Bhagat G, Chadburn A, Gaidano G, Mullighan CG, Rabadan R, Dalla-Favera R. Analysis of the coding genome of diffuse large B-cell lymphoma. Nat Genet. 2011; 43:830–837. [PubMed: 21804550]
10. Boice M, Salloum D, Mourcin F, Sanghvi V, Amin R, Oricchio E, Jiang M, Mottok A, Denis-Lagache N, Ciriello G, Tam W, Teruya-Feldstein J, de Stanchina E, Chan WC, Malek SN, Ennishi D, Brentjens RJ, Gascoyne RD, Cogné M, Tarte K, Wendel HG. Loss of the HVEM tumor suppressor in lymphoma and restoration by modified CAR-T cells. Cell. 2016; 167:405–418.e13. [PubMed: 27693350]

11. Okosun J, Wolfson RL, Wang J, Araf S, Wilkins L, Castellano BM, Escudero-Ibarz L, Al Seraihi AF, Richter J, Bernhart SH, Efeyan A, Iqbal S, Matthews J, Clear A, Guerra-Assunção JA, Bödör C, Quentmeier H, Mansbridge C, Johnson P, Davies A, Strefford JC, Packham G, Barrans S, Jack A, Du M-Q, Calaminici M, Lister TA, Auer R, Montoto S, Gribben JG, Siebert R, Chelala C, Zoncu R, Sabatini DM, Fitzgibbon J. Recurrent mTORC1-activating RRAGC mutations in follicular lymphoma. Nat Genet. 2016; 48:183–186. [PubMed: 26691987]
12. Kridel R, Sehn LH, Gascoyne RD. Pathogenesis of follicular lymphoma. J Clin Invest. 2012; 122:3424–3431. [PubMed: 23023713]
13. Tilly H, Rossi A, Stamatoullas A, Lenormand B, Bigorgne C, Kunlin A, Monconduit M, Bastard C. Prognostic value of chromosomal abnormalities in follicular lymphoma. Blood. 1994; 84:1043–1049. [PubMed: 8049424]
14. Compagno M, Lim WK, Grunn A, Nandula SV, Brahmachary M, Shen Q, Bertoni F, Ponzoni M, Scandurra M, Califano A, Bhagat G, Chadburn A, Dalla-Favera R, Pasqualucci L. Mutations of multiple genes cause deregulation of NF-κB in diffuse large B-cell lymphoma. Nature. 2009; 459:717–721. [PubMed: 19412164]
15. Oricchio E, Nanjangud G, Wolfe AL, Schatz JH, Mavrakis KJ, Jiang M, Liu X, Bruno J, Heguy A, Olshen AB, Socci ND, Teruya-Feldstein J, Weis-Garcia F, Tam W, Shaknovich R, Melnick A, Himanen JP, Chaganti RSK, Wendel HG. The Eph-receptor A7 is a soluble tumor suppressor for follicular lymphoma. Cell. 2011; 147:554–564. [PubMed: 22036564]
16. Zender L, Xue W, Zuber J, Semighini CP, Krasnitz A, Ma B, Zender P, Kubicka S, Luk JM, Schirmacher P, McCombie WR, Wigler M, Hicks J, Hannon GJ, Powers S, Lowe SW. An oncogenomics-based in vivo RNAi screen identifies tumor suppressors in liver cancer. Cell. 2008; 135:852–864. [PubMed: 19012953]
17. Chantranupong L, Wolfson RL, Orozco JM, Saxton RA, Scaria SM, Bar-Peled L, Spooner E, Isasa M, Gygi SP, Sabatini DM. The Sestrins interact with GATOR2 to negatively regulate the amino-acid-sensing pathway upstream of mTORC1. Cell Rep. 2014; 9:1–8. [PubMed: 25263562]
18. Parmigiani A, Nourbakhsh A, Ding B, Wang W, Kim YC, Akopiants K, Guan KL, Karin M, Budanov AV. Sestrins inhibit mTORC1 kinase activation through the GATOR complex. Cell Rep. 2014; 9:1281–1291. [PubMed: 25457612]
19. Peng M, Yin N, Li MO. Sestrins function as guanine nucleotide dissociation inhibitors for Rag GTPases to control mTORC1 signaling. Cell. 2014; 159:122–133. [PubMed: 25259925]
20. Budanov AV, Karin M. p53 target genes sestrin1 and sestrin2 connect genotoxic stress and mTOR signaling. Cell. 2008; 134:451–460. [PubMed: 18692468]
21. Bouska A, McKeithan TW, Deffenbacher KE, Lachel C, Wright GW, Iqbal J, Smith LM, Zhang W, Kucuk C, Rinaldi A, Bertoni F, Fitzgibbon J, Fu K, Weisenburger DD, Greiner TC, Dave BJ, Gascoyne RD, Rosenwald A, Ott G, Campo E, Rimsza LM, Delabie J, Jaffe ES, Braziel RM, Connors JM, Staudt LM, Chan WC. Genome-wide copy-number analyses reveal genomic abnormalities involved in transformation of follicular lymphoma. Blood. 2014; 123:1681–1690. [PubMed: 24037725]
22. Oricchio E, Ciriello G, Jiang M, Boice MH, Schatz JH, Heguy A, Viale A, de Stanchina E, Teruya-Feldstein J, Bouska A, McKeithan T, Sander C, Tam W, Seshan VE, Chan WC, Chaganti RSK, Wendel HG. Frequent disruption of the RB pathway in indolent follicular lymphoma suggests a new combination therapy. J Exp Med. 2014; 211:1379–1391. [PubMed: 24913233]
23. Mermel CH, Schumacher SE, Hill B, Meyerson ML, Beroukhim R, Getz G. GISTIC2.0 facilitates sensitive and confident localization of the targets of focal somatic copy-number alteration in human cancers. Genome Biol. 2011; 12:R41. [PubMed: 21527027]
24. Mavrakis KJ, Wolfe AL, Oricchio E, Palomero T, de Keersmaecker K, McJunkin K, Zuber J, James T, Khan AA, Leslie CS, Parker JS, Paddison PJ, Tam W, Ferrando A, Wendel HG. Genome-wide RNA-mediated interference screen identifies miR-19 targets in Notch-induced T-cell acute lymphoblastic leukaemia. Nat Cell Biol. 2010; 12:372–379. [PubMed: 20190740]
25. Jiang Y, Ortega-Molina A, Geng H, Ying HY, Hatzi K, Parsa S, McNally D, Wang L, Doane AS, Agirre X, Teater M, Meydan C, Li Z, Poloway D, Wang S, Ennishi D, Scott DW, Stengel KR, Kranz JE, Holson E, Sharma S, Young JW, Chu CS, Roeder RG, Shaknovich R, Hiebert SW, Gascoyne RD, Tam W, Elemento O, Wendel HG, Melnick AM. CREBBP inactivation promotes

the development of HDAC3-dependent lymphomas. Cancer Discov. 2017; 7:38–53. [PubMed: 27733359]

26. Schatz JH, Oricchio E, Wolfe AL, Jiang M, Linkov I, Maragulia J, Shi W, Zhang Z, Rajasekhar VK, Pagano NC, Porco JA, Teruya-Feldstein J, Rosen N, Zelenetz AD, Pelletier J, Wendel HG. Targeting cap-dependent translation blocks converging survival signals by AKT and PIM kinases in lymphoma. J Exp Med. 2011; 208:1799–1807. [PubMed: 21859846]
27. Egle A, Harris AW, Bath ML, O'Reilly L, Cory S. VavP-Bcl2 transgenic mice develop follicular lymphoma preceded by germinal center hyperplasia. Blood. 2004; 103:2276–2283. [PubMed: 14630790]
28. Shaknovich R, Geng H, Johnson NA, Tsikitas L, Cerchietti L, Greally JM, Gascoyne RD, Elemento O, Melnick A. DNA methylation signatures define molecular subtypes of diffuse large B-cell lymphoma. Blood. 2010; 116:e81–e89. [PubMed: 20610814]
29. Béguelin W, Popovic R, Teater M, Jiang Y, Bunting KL, Rosen M, Shen H, Yang SN, Wang L, Ezponda T, Martinez-Garcia E, Zhang H, Zheng Y, Verma SK, McCabe MT, Ott HM, Van Aller GS, Kruger RG, Liu Y, McHugh CF, Scott DW, Chung YR, Kelleher N, Shaknovich R, Creasy CL, Gascoyne RD, Wong KK, Cerchietti L, Levine RL, Abdel-Wahab O, Licht JD, Elemento O, Melnick AM. EZH2 is required for germinal center formation and somatic EZH2 mutations promote lymphoid transformation. Cancer Cell. 2013; 23:677–692. [PubMed: 23680150]
30. Bödör C, Grossmann V, Popov N, Okosun J, O'Riain C, Tan K, Marzec J, Araf S, Wang J, Lee AM, Clear A, Montoto S, Matthews J, Iqbal S, Rajnai H, Rosenwald A, Ott G, Campo E, Rimsza LM, Smeland EB, Chan WC, Braziel RM, Staudt LM, Wright G, Lister TA, Elemento O, Hills R, Gribben JG, Chelala C, Matolcsy A, Kohlmann A, Haferlach T, Gascoyne RD, Fitzgibbon J. EZH2 mutations are frequent and represent an early event in follicular lymphoma. Blood. 2013; 122:3165–3168. [PubMed: 24052547]
31. Morin RD, Mungall K, Pleasance E, Mungall AJ, Goya R, Huff RD, Scott DW, Ding J, Roth A, Chiu R, Corbett RD, Chan FC, Mendez-Lago M, Trinh DL, Bolger-Munro M, Taylor G, Hadj Khodabakhshi A, Ben-Neriah S, Pon J, Meissner B, Woolcock B, Farnoud N, Rogic S, Lim EL, Johnson NA, Shah S, Jones S, Steidl C, Holt R, Birol I, Moore R, Connors JM, Gascoyne RD, Marra MA. Mutational and structural analysis of diffuse large B—cell lymphoma using whole—genome sequencing. Blood. 2013; 122:1256–1265. [PubMed: 23699601]
32. Kridel R, Chan FC, Mottok A, Boyle M, Farinha P, Tan K, Meissner B, Bashashati A, McPherson A, Roth A, Shumansky K, Yap D, Ben-Neriah S, Rosner J, Smith MA, Nielsen C, Giné E, Telenius A, Ennishi D, Mungall A, Moore R, Morin RD, Johnson NA, Sehn LH, Tousseyn T, Dogan A, Connors JM, Scott DW, Steidl C, Marra MA, Gascoyne RD, Shah SP. Histological transformation and progression in follicular lymphoma: A clonal evolution study. PLOS Med. 2016; 13:e1002197. [PubMed: 27959929]
33. Sablina AA, Budanov AV, Ilyinskaya GV, Agapova LS, Kravchenko JE, Chumakov PM. The antioxidant function of the p53 tumor suppressor. Nat Med. 2005; 11:1306–1313. [PubMed: 16286925]
34. Rodrik-Outmezguine VS, Okaniwa M, Yao Z, Novotny CJ, McWhirter C, Banaji A, Won H, Wong W, Berger M, de Stanchina E, Barratt DG, Cosulich S, Klinowska T, Rosen N, Shokat KM. Overcoming mTOR resistance mutations with a new-generation mTOR inhibitor. Nature. 2016; 534:272–276. [PubMed: 27279227]
35. Boi M, Zucca E, Inghirami G, Bertoni F. PRDM1/BLIMP1: A tumor suppressor gene in B and T cell lymphomas. Leuk Lymphoma. 2015; 56:1223–1228. [PubMed: 25115512]
36. Bar-Peled L, Schweitzer LD, Zoncu R, Sabatini DM. Ragulator is a GEF for the rag GTPases that signal amino acid levels to mTORC1. Cell. 2012; 150:1196–1208. [PubMed: 22980980]
37. McCabe MT, Ott HM, Ganji G, Korenchuk S, Thompson C, Van Aller GS, Liu Y, Graves AP, Della Pietra A III, Diaz E, LaFrance LV, Mellinger M, Duquenne C, Tian X, Kruger RG, McHugh CF, Brandt M, Miller WH, Dhanak D, Verma SK, Tummino PJ, Creasy CL. EZH2 inhibition as a therapeutic strategy for lymphoma with EZH2-activating mutations. Nature. 2012; 492:108–112. [PubMed: 23051747]
38. Ritchie ME, Phipson B, Wu D, Hu Y, Law CW, Shi W, Smyth GK. *limma* powers differential expression analyses for RNA-sequencing and microarray studies. Nucleic Acids Res. 2015; 43:e47. [PubMed: 25605792]

39. Langmead B, Salzberg SL. Fast gapped-read alignment with Bowtie 2. Nat Methods. 2012; 9:357–359. [PubMed: 22388286]

40. Li H, Handsaker B, Wysoker A, Fennell T, Ruan J, Homer N, Marth G, Abecasis G, Durbin R. 1000 Genome Project Data Processing Subgroup, The Sequence Alignment/Map format and SAMtools. Bioinformatics. 2009; 25:2078–2079. [PubMed: 19505943]

41. Adriaens ME, Prickaerts P, Chan-Seng-Yue M, van den Beucken T, Dahlmans VEH, Eijssen LM, Beck T, Wouters BG, Voncken JW, Evelo CTA. Quantitative analysis of ChIP-seq data uncovers dynamic and sustained H3K4me3 and H3K27me3 modulation in cancer cells under hypoxia. Epigenetis Chromatin. 2016; 9:48.

42. Ortega-Molina A, Boss IW, Canela A, Pan H, Jiang Y, Zhao C, Jiang M, Hu D, Agirre X, Niesvizky I, Lee JE, Chen HT, Ennishi D, Scott DW, Mottok A, Hother C, Liu S, Cao XJ, Tam W, Shaknovich R, Garcia BA, Gascoyne RD, Ge K, Shilatifard A, Elemento O, Nussenzweig A, Melnick AM, Wendel HG. The histone lysine methyltransferase KMT2D sustains a gene expression program that represses B cell lymphoma development. Nat Med. 2015; 21:1199–1208. [PubMed: 26366710]

43. Wendel HG, de Stanchina E, Fridman JS, Malina A, Ray S, Kogan S, Cordon-Cardo C, Pelletier J, Lowe SW. Survival signalling by Akt and eIF4E in oncogenesis and cancer therapy. Nature. 2004; 428:332–337. [PubMed: 15029198]

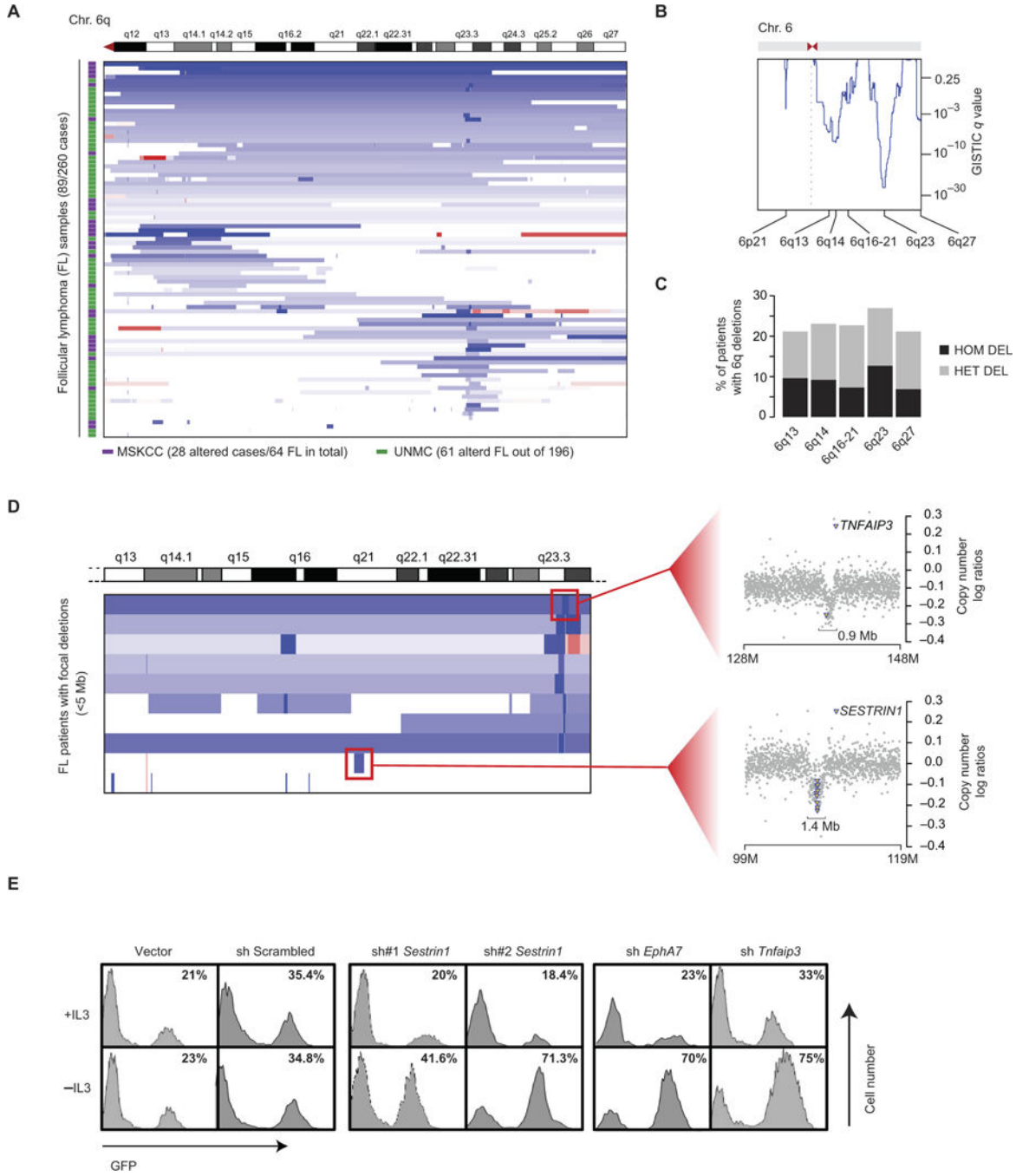

Fig. 1. Genomic analyses and a genetic screen identify *SESTRIN1* as a functional target of Chr. 6q deletions in FL

(**A**) Integrative Genome View of Chr. 6q deletions occurring in 34% (89 of 260) of FL tumors. (**B**) Analysis of recurrent deletions in Chr. 6 in FL using GISTIC algorithm. (**C**) Frequency of homozygous and heterozygous deletions in Chr. 6q. (**D**) Integrative Genome View visualization of 10 of 260 cases with focal deletions (<5 Mb) on Chr. 6q. Representative FL case with focal deletion affecting *SESTRIN1* and *TNFAIP3* locus is shown in detail. (E) Flow cytometry validation of individual shRNAs linked to green

fluorescent protein (GFP) showing percentages of GFP-positive cells before and after IL-3 withdrawal in pro–B cells transduced with the indicated constructs.

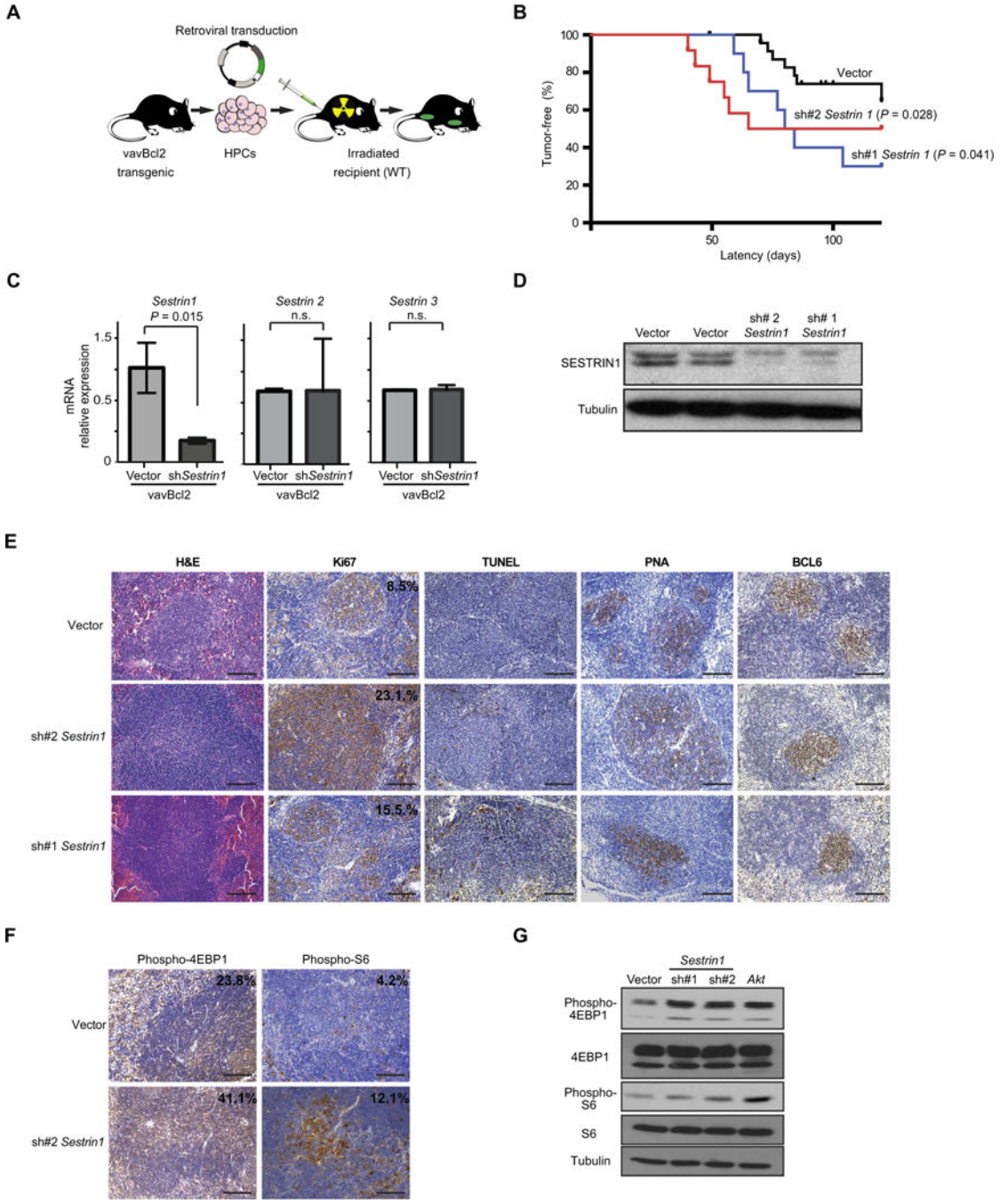

Fig. 2. Loss of Sestrin1 promotes FL development in vivo

(**A**) Graphic representation of chimeric mouse model based on the transplantation of vavBcl2 transgenic hematopoietic progenitor cells. WT, wild type. (**B**) Analysis of tumor latency in the vavBcl2 chimeric mouse model with sh-1 *Sestrin1* (blue; $n = 10$), sh-2 *Sestrin1* (red; $n = 12$), and vector (black; $n = 24$). Significant difference in survival was measured by log-rank test between animals expressing empty vector and shRNAs targeting *Sestrin1*. (**C** and **D**) Characterization of the shRNAs against Sestrin1. (C) *Sestrin1*, *Sestrin2*, and *Sestrin3* mRNA expression in tumors expressing vector or shRNA for *Sestrin1*. *P* values

were calculated using two-tailed *t* test. n.s., nonsignificant ($P < 0.05$). Data are shown as a bar graph corresponding to the mean ± SD. (D) Immunoblot analysis in pro—B cells expressing shRNA for *Sestrin1* or vector. The antibody recognized two Sestrin1 isoforms, and they were both targeted by shRNA. (**E**) Representative images of immunohistochemistry and histopathology analyses of indolent vavBcl2 tumors expressing shRNAs against *Sestrin1*. Ki67 quantification was performed on three different slides for each tumor type using ImageJ. Scale bars, 100 μm. H&E, hematoxylin and eosin; PNA, peanut agglutinin; BCL6, B cell lymphoma 6. (**F**) Representative immunohistochemistry analyses of phospho-S6 and phospho-4EBP1 in vavBcl2 tumors expressing vector or shRNA #2 for Sestrin1. Quantification was performed on two different slides for each tumor type using ImageJ. Scale bars, 100 μm. (**G**) Analysis of phosphorylation of S6 and 4EBP1 by Western blot in B cells expressing vector, short hairpin for Sestrin1, or overexpressing *Akt* as control.

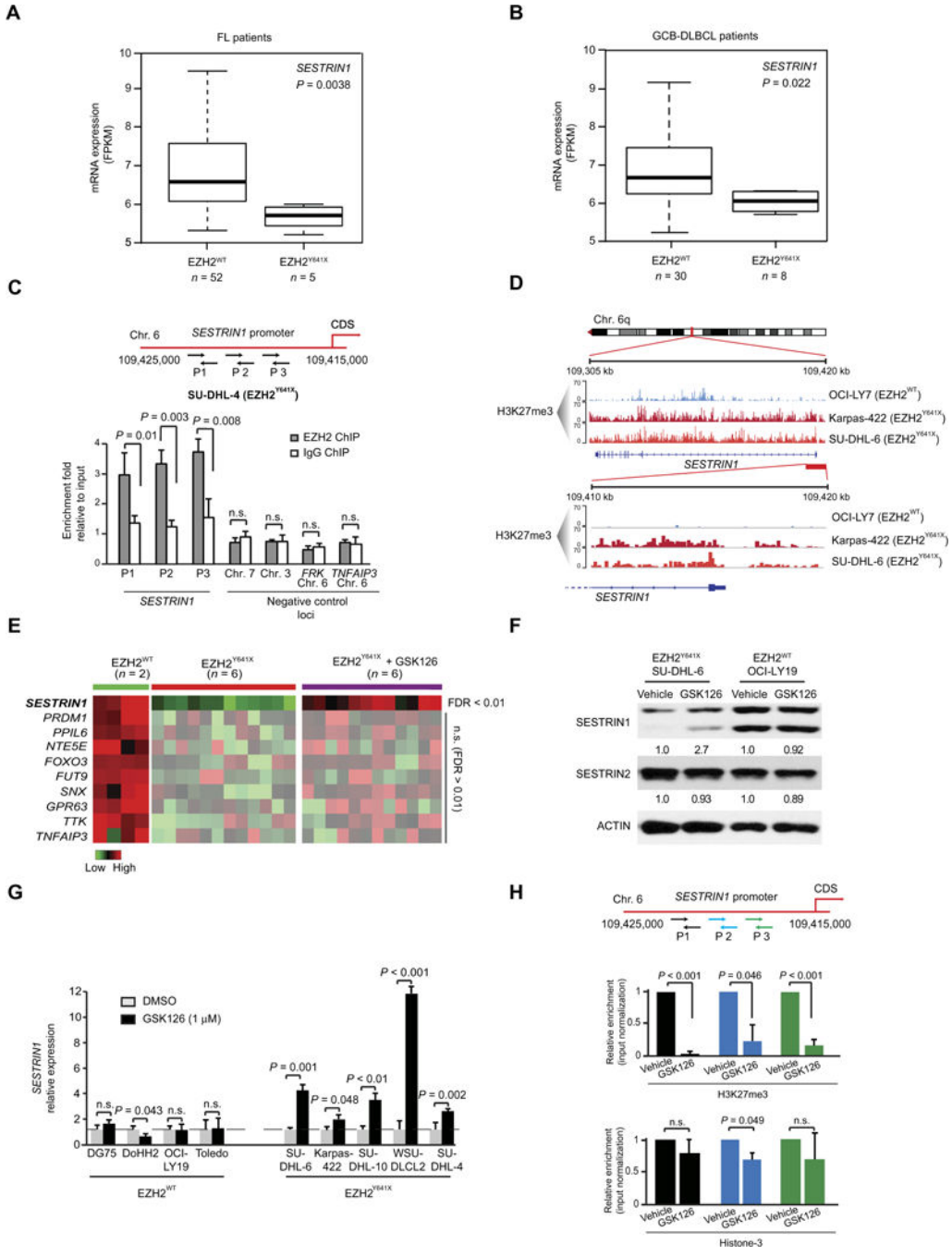

Fig. 3. *SESTRIN1* is a direct target of EZH2^{Y641X} silencing in lymphomas

(**A**) Differential *SESTRIN1* expression in 57 primary FL samples with and without EZH2^{Y641X} mutation. The *P* value was calculated by Wilcoxon test. Data are shown using the R boxplot function with whiskers extending to minimum and maximum values. FPKM, fragments per kilobase million. (**B**) Differential *SESTRIN1* expression in 38 germinal center B cell—DLBCL (GCB-DLBCL) samples, including 8 samples with the EZH2^{Y641X} gain-of-function mutation. The *P* value was calculated by Wilcoxon test. Data are shown using the R boxplot function with whiskers extending to minimum and maximum values. (**C**) ChIP

for EZH2 and immunoglobulin G (IgG) in SU-DHL-4 lymphoma cell lines, followed by qPCR (ChIP-qPCR) using three primers spanning *SESTRIN1* promoter (P1, P2, and P3), two negative control primers mapping on Chr. 6 upstream of FRK and TNFAIP3 coding sequence (CDS), and two other negative controls mapping on Chr. 7 and Chr. 3. Data are shown as a bar graph corresponding to the mean ± SEM. (**D**) H3K27me3 ChiP sequencing (ChIP-seq) signal spanning *SESTRIN1* genomic locus (Chr. 6: 109,305,000 to 109,420,000) in OCI-LY7 $EZH2^{WT}$ cells (light blue) and Karpas-422 (dark red) and SU-DHL-6 (red) $EZH2^{Y641X}$ mutant cells. Bottom: Zoomin in SESTRIN1 promoter and coding start site region (Chr. 6: 109,410,000 to 109,420,000). (**E**) Differential expression analysis focused on genes within the Chr. 6q region in $EZH2^{WT}$ lymphoma cell lines ($n = 2$), $EZH2^{Y641X}$-mutated ($n = 6$), and mutated lines treated with the EZH2 inhibitor GSK126 for 72 hours ($n = 6$ $EZH2^{Y641X}$ + GSK126). Each cell line has been analyzed in duplicate. *SESTRIN1* is significantly differentially expressed between the three groups (FDR < 0.01). (**F**) Western blot analysis of SESTRIN1 and SESTRIN2 in $EZH2^{Y641X}$ (SU-DHL-6) and $EZH2^{WT}$ (OCI-LY19) lymphoma cell lines treated with the EZH2 inhibitor (1 μM GSK126 for 72 hours). Sestrin1 antibody detects two SESTRIN1 predicted isoforms. Quantification was performed using Image Studio Lite, and the average of the signal intensity was normalized to the control. (**G**) *SESTRIN1* expression in the indicated $EZH2^{WT}$ and $EZH2^{Y641X}$-mutated lymphoma cell lines treated for 72 hours with dimethyl sulfoxide (DMSO) or 1 μM GSK126. Data are shown as a bar graph corresponding to the mean ± SEM. (**H**) ChIP for H3K27me3 and histone-3 in SU-DHL-6 lymphoma cell line with and without GSK126 (1 μM for 72 hours), showing loss of *SESTRIN1* promoter binding upon EZH2 inhibition. Data are shown as a bar graph corresponding to the mean ± SEM.

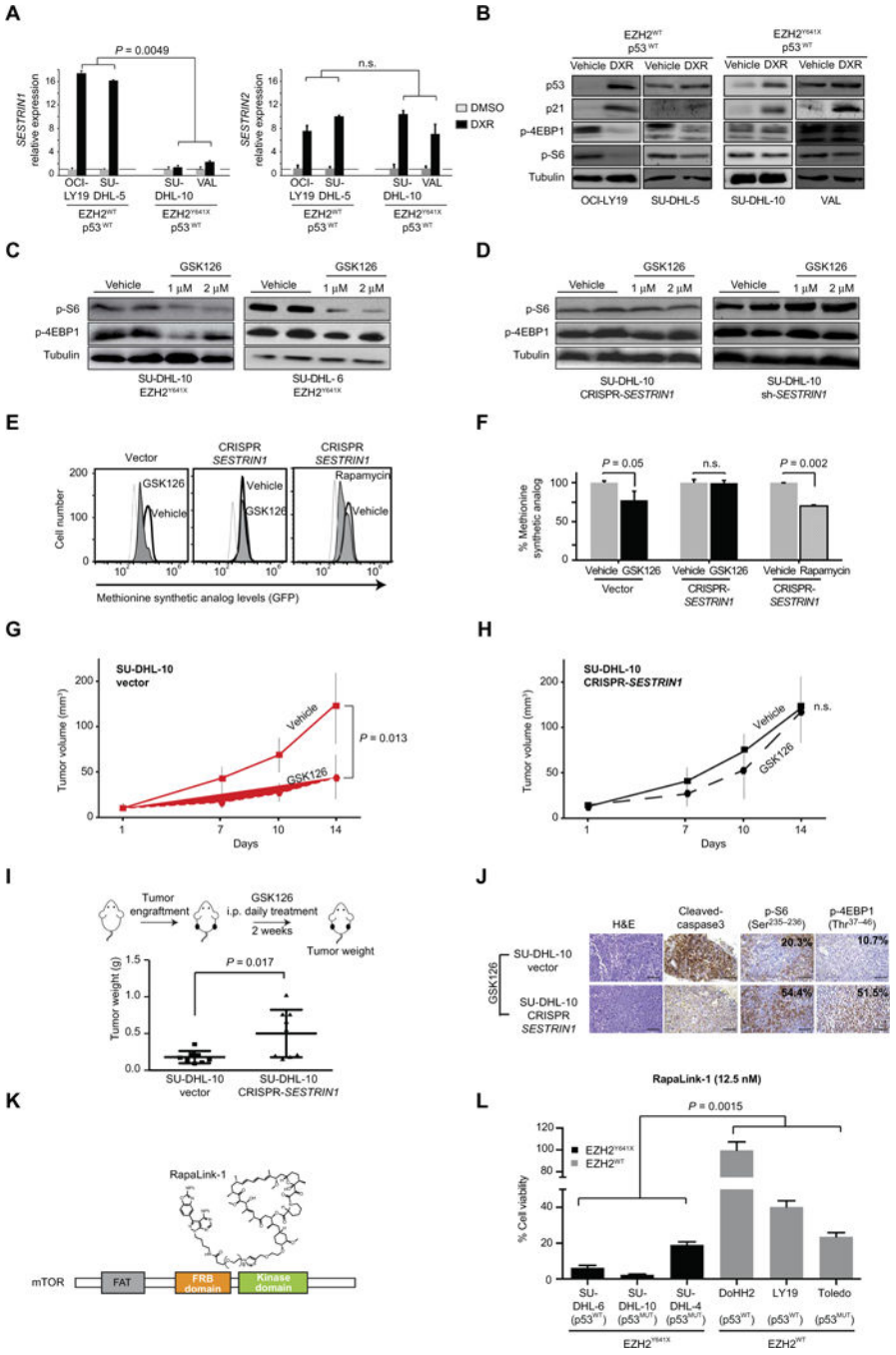

Fig. 4. *SESTRIN1* determines the effects of EZH2 inhibition in lymphoma

(**A**) *SESTRIN1* and *SESTRIN2* expression in OCI-LY19 and SU-DHL-5 lymphoma cells ($EZH2^{WT}/p53^{WT}$) and SU-DHL-10 and VAL cells ($EZH2^{Y641X}/p53^{WT}$) treated with DXR or vehicle for 6 hours. Two-tailed *t* test was used to define significant ($P < 0.05$) or nonsignificant ($P > 0.05$) difference between $EZH2^{WT}$ and $EZH2^{Y641X}$ mutant cells. Data are shown as a bar graph corresponding to the mean ± SEM. Each experiment had two or three technical replicates. (**B**) Immunoblot with the indicated antibodies in OCI-LY19 and SU-DHL-5 lymphoma cells ($EZH2^{WT}/p53^{WT}$) and SU-DHL-10 and VAL cells

(*EZH2*^{Y641X}/*p53*^{WT}) treated with DXR or vehicle for 6 hours. (**C**) Analysis of S6 and 4EBP1 phosphorylation in *EZH2*^{Y641X}-mutated lymphoma cell lines SU-DHL-10 and SU-DHL-6 treated for 72 hours with DMSO (vehicle), or 1 or 2 μM GSK126. (**D**) Immunoblot to assess S6 and 4EBP1 phosphorylation in SU-DHL-10 cells with mutations in *SESTRIN1* genomic locus (CRISPR-*SESTRIN1*) or expressing shRNA targeting *SESTRIN1* (sh-*SESTRIN1*) treated with vehicle (DMSO) or GSK126 (1 or 2 μM for 72 hours). (**E**) Flow cytometry analysis to measure methionine analog (AHA) incorporation in lymphoma cells treated with the EZH2 inhibitor (GSK126) or rapamycin with or without SESTRIN1. (**F**) Quantification of the methionine synthetic analog incorporation. Data are shown as a bar graph corresponding to the mean ± SD. (**G** and **H**) Tumor growth curves of xenografted SU-DHL-10 expressing vector (G) or CRISPR-*SESTRIN1* (H), treated for 14 days with vehicle or GSK126. The mean tumor volumes ± SD are expressed in cubic millimeter. *P* values were calculated by twotailed *t* test. n.s., nonsignificant difference ($P > 0.05$). (**I**) Tumor weight in animals xenografted with SU-DHL-10 cells expressing vector or single-guide RNA (sgRNA) targeting *SESTRIN1* (CRISPR-*SESTRIN1*) and treated with the EZH2 inhibitor (75 mg/kg ip) for 14 days. *P* value was calculated by paired *t* test. Data are shownassingle values with mean ± SD. (**J**) Representative images of immunohistochemistry and histopathology analyses of xenografted tumors expressing vector or sgRNA targeting Sestrin1 (CRISPR-*SESTRIN1*) and stained for cleaved caspase3, phospho-S6, and phospho-4EBP1. Quantification was performed with ImageJ. Scale bars, 200 μm. (**K**) Graphic representation of RapaLink-1 molecular structure and the FAT (FRAP-ATM-TTRAP), FRB, and kinase mTOR domains targeted by the inhibitor. (**L**) Percentage of viable cells in *EZH2*^{Y641X} mutant and *EZH2*^{WT} cells treated with the mTOR inhibitor (12.5 nM RapaLink-1) for 48 hours. Each cell line was analyzed in triplicate, and two-tailed *t* test was used to assess the significance of the difference in response between *EZH2*^{Y641X} mutant and *EZH2*^{WT} cells. Data are shown as a bar graph corresponding to the mean ± SD.